Metropolitan rail network robustness

Article *in* Physica A Statistical Mechanics and its Applications · February 2020

DOI: 10.1016/j.physa.2020.124317

CITATIONS
41

READS
388

2 authors:

Oded Cats
Delft University of Technology
300 PUBLICATIONS **6,744** CITATIONS

SEE PROFILE

Panchamy Krishnakumari
Delft University of Technology
28 PUBLICATIONS **390** CITATIONS

SEE PROFILE

Metropolitan Rail Network Robustness

Oded Cats
Department of Transportation and Planning
Delft University of Technology
P.O. Box 5048, 2600 GA Delft, The Netherlands
Phone number: +31 15 27 85279
Email: o.cats@tudelft.nl

Panchamy Krishnakumari
Department of Transportation and Planning
Delft University of Technology
P.O. Box 5048, 2600 GA Delft, The Netherlands
Phone number: +31 15 27 85279
Email: p.k.krishnakumari@tudelft.nl

Abstract

In large-scale urban agglomerations, heavy rail in the form of metro and commuter train serves as the backbone of the metropolitan public transport network. The objective of this paper is to investigate whether networks with strikingly different structure and development pattern exhibit different robustness properties in the event of random and targeted attacks. We adopt a complex network theory approach, investigating network performances under alternative sequential disruption scenarios corresponding to the successive closure of either stations or track segments. We also investigate the case where the removal of a network node or link implies the closure of all traversing lines. Network performance is measured both in terms of the capacity of the network to function in terms of connectivity as well as the additional impedance induced for those that remain connected. An aggregate robustness indicator based on the integral of the deterioration of network performance is adopted. Three exemplary networks are selected, the urban rail networks of London, Shanghai and Randstad. These three networks offer showcases of short and long development patterns, mono- and polycentric agglomeration structures, including the largest and the oldest metropolitan heavy rail networks. The polycentric network of the Randstad was found the least robust in this analysis when compared to the more monocentric networks of London and Shanghai. The London network is in general more robust than the Shanghai network thanks to the presence of cycles beyond the core. Our findings provide more nuanced evidence on the relation between network structure and development pattern, and its robustness.

Keywords: Transport Network; Robustness; Network Structure; Critical Infrastructure; Disruptions; Line Closure.

1 INTRODUCTION

Urban population increases rapidly worldwide as people are seeking better quality of life and job opportunities and governments stimulate agglomeration effects through investments in infrastructure. Faced with this situation, local authorities aim to improve mobility by densifying and expanding the respective public transport system. In large-scale urban agglomerations, heavy rail in the form of metro and commuter train serves as the primary high-level metropolitan public transport network (MPTN). Transport systems, including MPTN, are subject to recurrent disruptions that may result in severe consequences for network performance and the metropolitan metabolism as a whole. The robustness of critical infrastructure such as mass MPTNs is high on the planning and policy agenda (Homeland Security 2010). Notwithstanding, there is lack of knowledge on how network structure and design philosophy impacts its robustness. This study aims to contribute to this topic by adopting a complex network theory approach.

1.1 Network structure development

MPTN can be represented as a graph where stations correspond to nodes and track segments to links. Lin and Ban (2013) provide a review of the literature devoted to transport network topology and measures adopted from complex network perspective since the early 2000s. A large number of studies that examined MPTN worldwide concluded that they exhibit scale-free and small-world properties. The former implies that the degree of a graph follows a power-law distribution with the number of connections decreasing exponentially – i.e. few stations with many connections and many stations with few connections while the latter implies that any node can be reached within a few steps regardless of the size of the network and are thus efficient in transmitting information (Latora, 2001). The combination of these two properties is the blueprint of a hub and spoke network that branches out as you move away from the central core which Roth et al. (2012) found to characterize the world's largest subway systems. This can be expected to happen if network evolution, the process in which new stations and track segments are added to the network, follows a preferential attachment mechanism where new stations are more likely to be connected to other stations which are already well-connected (i.e. known as the rich getting richer phenomenon).

The structure of the public transport network is intertwined with the urban and regional development and the underlying policy making process. Metropolitan areas are often characterized as monocentric areas (as implied by the etymology of the word metropolitan) with radial networks. Notwithstanding, MPTN vary in the extent to which they are indeed concentrated around a single center with secondary centres being the norm rather than the exception. Louf and Barthelemy (2013) investigated the underlying process that yield an unstable monocentric regime that leads to the transition towards the growth of polycentric organizations.

The extent to which an urban agglomeration exhibits monocentric or polycentric land-use and travel patterns depends, among other things, on the underlying MPTN and the planning policy. The latter is also reflected in the development of MPTN which is an important driver in realizing such plans. Examples of the latter are the light rail projects in Paris and the on-going metro extension in Stockholm (Cats 2017), both of which have been devised to stimulate a more polycentric development. In several cases such as in the Randstad in the Netherlands, the Flemish diamond in Belgium and the Ruhr area in Germany, an agglomeration of cities which is not dominated by any one city.

All of the abovementioned networks have evolved over many decades and their structure and developments reflect the evolution in planning policies and realities. They are thus the outcome of the decisions of a large number of planners with none of them envisioning the current state of the network. In contrast, MPTN in large cities in China have developed swiftly with unprecedented investments. These rapid developments are the result of a masterplan that is overseen by the transport authority. For illustration, Shanghai, Guangzhou and Nanjing, which are the first, fourth and sixth longest metro networks in the world in terms of track-km, have seen the first line inaugurated in 1993, 1997 and 2005,

respectively. Metro systems in three more Chinese cities opened as recently as 2004-2005 and their network length already exceeds in length that of the Paris network. This strikingly different planning trajectory implies less path-dependence and reflects potentially a more cohesive network design approach which has been designed and implemented within a relatively short time span. Wang et al. (2009) stress the strong political influence and the importance of central governmental policies in network development and its impacts on changes in accessibility and the generation of economic centres in analyzing the accessibility impacts of the development of the Chinese railway network during the 20th century. It remains however unknown what are the consequences of these differences for network robustness.

1.2 Network robustness analysis

The complex network theory approach enables the robustness analysis of MPTN and the relation between the MPTN topology and its robustness. Ash and Newth (2007) developed an evolutionary model for link additions to a synthetic grid network and assessed the impacts of network design on the ability to withstand link failures. They concluded that the least vulnerable designs were characterized by the formation of a cluster of hubs that are highly inter-connected, enabling the re-distribution of flows in the event of disruptions. Derrible and Kennedy (2010a, 2010b) defined metrics that they believe are indicative of network robustness. They postulated using the number of cyclic paths available in the network since it approximates the possibility to use alternative routes under disruption. However, the relevance of this indicator in explaining network performance in the event of disruptions through experiments was not established. According to their criterion, the MPTN of Tokyo and Seoul are particularly robust followed by among others, Paris and London. Zhang et al. (2015) studied 17 generic network structures and concluded that redundancy is a key determinant of network capability to withstand disasters. While some insights can be gained from analyzing taxonomy of networks structures, real-world MPTN are complex and are comprised of a large number of diverse building blocks (e.g. hub-and-spoke, grid, ring, diamond etc.) which cannot be represented as direct extrapolation of their fundamental elements. Rodriguez-Nunez and Garcia-Palomares (2014) and Jenelius and Cats (2015) modelled the MPTN service network concluded that lines that offer many transfer opportunities to other lines such as ring and cross-radial lines are especially important in adding cycles and thus contributing to network robustness. This was indeed one of the goals of the polycentric development policy promoted by the respective planning authorities (Cats et al. 2015). Since a polycentric structure is reflected by a more distributed MPTN it can be expected to contribute to network robustness due to the more even distribution of network flows and the potentially lesser dependency on few critical network elements.

A systematic analysis of network robustness requires performing a full-scan of the impacts of failures on network performance. Wang et al. (2014) provide a review of the literature on vulnerability modelling of transportation networks for different modes and failure scenarios using various vulnerability indicators. In the field of MPTN, the studies of von Ferber et al. (2012) and Zhang et al. (2011) paved the way by examining the impact of a sequential failure of network elements – either nodes (stations) or links (track segments). In both studies, three strategies for determining the failure sequence were investigated – random, in descending order of node degree and in descending order of betweenness centrality. The former reflects random failures while the latter two are designed to examine network ability to withstand targeted attacks. Zhang et al. (2011) applied this approach to the network of Shanghai from 2010. von Ferber et al. (2012) applied the analysis to the networks of London and Paris. The results indicate that Paris is significantly more robust than London in the event of node degree removal strategy while the networks perform very similarly under the other two strategies. However, the analysis was performed for the entire public transport network, treating metro and bus lines as if they were indistinguishable. The abovementioned studies assumed that the impacts of the breakdown of a network element are encapsulated and confined to the respective element. However, in practice, the impacts of the breakdown may carry consequences that extend beyond the primary disruption and may sabotage operations further upstream or downstream. William and Musolesi (2016) developed a method for accounting for the

temporal suspension of the propagation of disruptions in spatial networks. Malandri et al. (2018) investigated the extent to which service disruptions propagate across the network in both time and space using a dynamic network loading model. Numerical experiments for the metro networks of Paris, London and New York indicate that attacks based on node betweenness centrality where most effective in harming the network. Pagani et al. (2019) employ topological indicators to assess network robustness and resilience for the London urban rail network.

1.3 Study objective and outline

The objective of this paper is to compare the robustness of selected public transport networks which exhibit different properties to both random and targeted attacks and gain insights on the role of network structure and its development pattern. To this end, three large rail networks in three exemplary agglomerations are selected –Shanghai, Randstad (the Netherlands) and London. These three networks offer showcases of short and long development patterns, mono- and polycentric agglomeration structures, including the largest and the oldest metropolitan heavy rail networks. These case study networks are selected due to their distinctive development trajectories, structures and properties in order to investigate the robustness of diverse metropolitan rail networks. Notwithstanding, the findings of this analysis are explorative rather than exhaustive given the peculiarity of transportation networks. Moreover, we explicitly consider and analyze the impacts of line closures due to node or link removals on network robustness. This goes beyond the state-of-the-art by considering the ramifications of infrastructure failure on service functionality and assessing the consequences for network robustness.

This paper is structured as follows. In the following section, we present the method and detail the network representation, failure scenarios and the measures used for quantifying network robustness. In section 3 we present our case study heavy rail networks of Shanghai, Randstad and London. Results are reported and analyzed in the section 4. The conclusion and network design implications are then discussed in section 5.

2 METHOD

2.1 Network representation and centrality indicators

The MPTN infrastructure is represented as a graph by representing each station as a node and introducing a link between each pair of stations that are directly connected by a track segment. This follows the so-called L-space representation (von Ferber et al. 2009). The physical MPTN is thus represented as an undirected graph $G(N, E)$ where the set N denotes rail stations and the link set $E \subseteq N \times N$ represents direct connections between stations. Each link may be operated by one or several public transport lines. A is the adjacency matrix of the graph G, where each entry in the matrix, a_{ij}, equals one if there is a link connecting stations $i, j \in N$ and is otherwise zero.

A line l is defined by a sequence of nodes, i.e. stops, $l = (n_{l,1}, n_{l,2}, \dots, n_{l,|l|})$ where all stops are members of N and the set of all lines is denoted L. We let $e \in l$ mean that link e is in line l, i.e., $e = (n_{l,i}, n_{l,i+1})$ for some i. Note that each node and link might be traversed by multiple lines.

Two measures of network centrality are used in this study, degree and betweenness and both are defined for both nodes and links. These two indicators are selected because they provide information on how well nodes are connected - degree is an indicator of local connectivity while betweenness measures global connectivity. The former indicates the extent of interchange opportunities whereas the latter pertains to volumes traversing the network element.

Node degree is the number of direct neighbors, hence directly connected stations, and is defined as

$$k_i = \sum_{j \in N} a_{ij} \quad \forall\, i \in N \tag{1}$$

where k_i is the degree of node i. Following the definition proposed in (von Ferber et al. 2012), link degree is defined as the sum of degrees of the nodes it connects minus its own contribution to their degrees, hence

$$k_e = k_{e^-} + k_{e^+} - 2 \quad \forall\, e \in E \tag{2}$$

Where e^- and e^+ denote the upstream and downstream nodes of link e, respectively.

Unlike degree centrality, betweenness centrality measures the role of the node or link in the network as a whole, not only in relation to its direct neighbors. Betweenness centrality is defined here in relative terms, as the share of shortest paths connecting origin-destination pairs in the network that traverse through a certain node or link. The formula for node betweenness centrality is

$$b_i = \sum_{j \in N; j \neq i} \sum_{k \in N, k \neq j} \frac{\sigma_{jk}(i)}{\sigma_{jk}} \tag{3}$$

where σ_{jk} is the number of shortest paths between nodes $j, k \in N$ and $\sigma_{jk}(i)$ is the number of these paths that go through node $i \in N$. And for link betweenness centrality

$$b_e = \sum_{j \in N} \sum_{k \in N, k \neq j} \frac{\sigma_{jk}(e)}{\sigma_{jk}} \tag{4}$$

where $\sigma_{jk}(e)$ is the number of shortest paths between nodes $j, k \in N$ that go through link $e \in E$.

The abovementioned indicators are used in determining the sequence in which disruption scenarios are simulated as described in the following sub-section.

2.2 Network element failure scenarios

Network elements – either nodes or links – can be subject to both random and malicious failures. Both stations and track segments may temporarily be closed due to construction or maintenance works, as well as unplanned closures due to technical or mechanical failures such as vehicle breakdowns and switch or signal failure. Other causes of unplanned disruptions are accidents, suicide attempts and terror-related threats and attacks. The latter typically affect stations.

The approach taken in this study is to simulate a sequence of link or node failures. Each scenario involves the sequential removals of either nodes or links. In the search for the most devastating effect, the perpetrators of a targeted attack are assumed to target network elements that are most heavily loaded and that will result with the most adverse conditions. Such scenarios were simulated in previous works such as von Ferber et al. (2012) and Pagani et al. (2019) in order to eaxmine the most severe network degradation cirucmstances. Degree centrality and betweenness centrality are therefore used as a possible attack strategy. Note that the removal of a node or link results in a new (reduced) network which affects the centrality indicators for the remaining nodes and links. The metrics are therefore recalculated and updated after each removal step in order to ensure that the most central network element is selected to be removed in the successive step.

Random attacks involve the random removal of links or nodes, each one picked in random from the remaining set of links or nodes. Crucially, the order in which links or nodes are removed may have great consequences for network performance due to both the specific elements selected as well as path dependency in the removal sequence. Neither the analysis in (von Ferber et al. 2012) nor (Zhang et al. 2011)

report how the random removal strategy was precisely performed. In order to attain meaningful results, a number of simulation runs needs to be performed. At the same time, the number of possible sequences is prohibitive even for fairly small networks. We assure statistically robust results by running a number of random removal sequences and then determining how many such replications are needed to attain a statistically significant result within a high (i.e. 95%) level of confidence.

The following pseudocode describes the implementation of node removal strategies with the link removal strategies following a similar procedure.

Algorithm 1: **Node removal strategies**

Input: **Rail station list *N*, edge list *E*, *strategy***
Output: **Network robustness measures**
$E_r \leftarrow E$, $N_r \leftarrow N$
while $|N_r| == 0$ **do**
    if strategy == degree
        calculate node degree k of $G(N_r, E_r)$
        $[k_r, order] \leftarrow$ DescendingSort(k)
        $N_r \leftarrow N_r[order]$
        $i \leftarrow N_r[1]$
    if strategy == betweenness
        calculate node betweenness b of $G(N_r, E_r)$
        $[b_r, order] \leftarrow$ DescendingSort(b)
        $N_r \leftarrow N_r[order]$
        $i \leftarrow N_r[1]$
    if strategy == random
        generate random number $1<m<|N_r|$
        $i \leftarrow N_r[m]$
    $E_r \leftarrow E_r - \{a_{ij}, a_{ki}\}$ //Remove edges from the graph with node *i* as incoming or outgoing nodes
    $N_r \leftarrow N_r - \{i\}$ //Remove node *i* from the graph
    calculate network robustness measures of updated $G(N_r, E_r)$

The abovementioned network element failure scenarios imply that the impacts of the breakdown of a network element are encapsulated and confined to the respective element. This may indeed be the case when short-turning is possible (i.e. switches are available) at the immediate upstream and downstream stations of the disrupted link or all incoming and outgoing links from a disrupted station. However, in practice, the impacts of the breakdown of a track segment or the closure of a station may have more adverse consequences for service operations. For example, a suspected item or a suicide attempt at either a station or a track segment is likely to sabotage the operations of all services traversing the respective network element. Rail-bound services are especially prone to such ramifications due to the limited availability to bypass the disrupted segment, thus hampering the operations of all services traversing the network element.

We therefore test an additional set of scenarios corresponding to each of the successive removal strategies described above. For each of these scenarios, the removal of a network node or link implies the closure of all service lines - along with all their stations and track segments - traversing the respective network elements. Formally, the removal of node n_i implies the shutdown of all lines that traverse the node $\{l \in L_{n_i}: n_i \in l\}$ and consequently the removal of the respective nodes $\{n \in N_i: n \in l_i; l_i \in L_{n_i}\}$ and links $\{e \in E_i: e \in l_i; l_i \in L_{n_i}\}$. The same approach is applied in the event of a link removal.

In summary, twelve failure scenarios are analyzed; the combination of three successive removal strategies – random, degree and betweenness, each of which applied to either nodes or links, and each of which with or without the shutdown of all line operations . The following sub-sections describe the network robustness indicators calculated to assess the impact of the failure scenarios.

2.3 Network performance and robustness indicators

System robustness is defined in the context of this study as system's ability to maintain its functionality under disruptions. In the context of MPTN, the core function of the system is to enable users to travel efficiently between different parts of the network. Various measures can be used to quantify network performance. Network robustness is then assessed by comparing the network performance under disruption to the original undisrupted performance.

We use two indicators to describe network performance, pertaining to the ability to travel and the detour inflicted by the disrupted situation. The former is assessed by identifying the largest sub-network that remains intact and measuring its size in relation to the original (complete) network size, or mathematically

$$S(r^n) = \frac{|N_r|}{|N|} \text{ or } S(r^e) = \frac{|E_r|}{|E|} \quad (5)$$

where $S(\cdot)$ is the *Relative Size* of the largest connected sub-network in removal step r^n or r^e of removing nodes or links, respectively. N_r (or E_r) is the set of nodes (or links) that remained in step r. The larger the sub-network is, the more likely it is that one can travel between a given origin-destination pair.

Even if it is still possible to travel using the MPTN between a given origin and destination, the removal of nodes or links may require performing detours and hence induce additional impedance. To enhance the realism of the robustness analysis performed, the second network performance indicator is designed to assess this effect. The average shortest path length is commonly used as a network efficiency indicator since it captures network transition capability. In order to realize the objective of this study of comparing different networks, the normalized average shortest path, $\hat{l}$, is calculated using the following equation:

$$\hat{l} = \frac{2}{|N|(|N|-1)} \sum_{i \in N} \sum_{j \in N, i \neq j} l_{ij} \quad (6)$$

where $\langle l \rangle$ is the mean shortest path length and l_{ij} is the length of a shortest path between nodes i and j (here, the number of stations that need to be traversed).

Similar to the relative size metric, network performance under a given disruption state can be then assessed in terms of its deterioration compared to the original state, denoted by $\tilde{l}$, as follows:

$$\tilde{l}(r^n) = \frac{\hat{l}(r^n)}{\max\limits_{i,j} l_{ij}(0)} \quad \text{or} \quad \tilde{l}(r^e) = \frac{\hat{l}(r^e)}{\max\limits_{i,j} l_{ij}(0)} \quad (7)$$

Where $\hat{l}(\cdot)$ is the Normalized Average Shortest Path in a certain removal step r^n or r^e with the undisrupted initial phase denoted by zero. In the course of removal steps, the network may not remain intact anymore. The original case here pertains to the longest rather than the average shortest path. A problem with the $\hat{l}$ metric arises when a pair of nodes is totally disconnected as this will result in infinite value of the mean shortest path. In this study, the infinite value is replaced by the 'diameter' of the network, i.e. the maximal shortest path length, in the initial undisrupted network. Hence, in case there is no path available between an Origin-Destination pair, $l_{ij}(\cdot) = \max\limits_{i,j} l_{ij}(0)$.

The two network performance indicators can be calculated for the network resulting from each removal step. This allows analyzing how performance losses evolve over the course of the sequence of removals and what was coined by Cats et al. (2017) the degrading rapidity. This is especially useful for identifying how long the network remains robust to disruption, whether there is a transition point and the overall trend. It is however also desirable to quantify the overall robustness by considering the accumulated effect of disruption of different scenarios on different MPTN. To this end, following Cats et al. (2017), the integral over $S(\cdot)$ in relation to the sequence of increasingly disrupted networks (from $|N_r| = \{|N|, |N|-1, \dots, 0\}$, can be calculated. The larger the value the more robust the network is

$$A = 100 \cdot \int_0^1 S(\cdot) \quad (8)$$

$A = [0,1]$, where 0 is the most vulnerable and 1 is the most robust.

The following section describes the networks to which this method is applied.

3 APPLICATION

The 2018 heavy rail networks of Shanghai, the Randstad and London, constitute the three case study networks. These three large networks are selected because they are exemplary of a rapid and more centralized development, a polycentric and decentralized development, and a monocentric and continuous development spanning over a long period of time, respectively. London and Shanghai come at fourth and ninth place respectively among world's 15 largest MPTN in terms of the complexity as studied by Gallotti et al. (2016). We choose to investigate only the heavy-rail network so that network links have an equivalent capacity and thus reflect reasonable routing alternatives in the event of a disruption. In all cases, the (light, metro, commuter and intercity) rail services operate with joint frequencies of 10-30 trains per hour on the main corridors. The train traffic and the respective demand can thus be assumed to be possibly absorbed. This aspect has been overlooked in studies that included links of different modal hierarchy such as regional train and metro along with tram and bus in the same graph representation (e.g. Zhang et al. 2011). Note that the metro networks of London and Shanghai were found by Wang et al. (2017) to be roughly equally robust using a series of topological robustness indicators.

Shanghai is a fast growing city and is a global business hub with the metropolitan area encompassing more than 24 million inhabitants. Shanghai is characterized by a monocentric development pattern. The MPTN consists of the rapidly developing metro network which is now the most extensive network in terms of track length in the world with 200km of metro tracks currently under construction.

The Randstad area is a megapolis, an urban agglomeration in the west of the Netherlands which extends into four provinces: North Holland, Flevoland, South Holland and Utrecht. The total population amounts to 8 million and includes the four largest cities of the Netherlands: Amsterdam, Rotterdam, The Hague and Utrecht. The MPTN consists of the inter-city and regional rail connections characterized by high frequencies and relatively short inter-station distances as well as metro services which are centered around Amsterdam and Rotterdam, including a metro-light rail line connecting the cities of Rotterdam and The Hague.

London is the center of a metropolitan area in which 14 million people reside. The metropolitan London heavy-rail network includes the underground, overground and Transport for London Rail. London underground, the world's first, opened in 1863. London overground is a suburban train developed with the concept of orbital services around London. TfL Rail comprises of two east-west railway lines (which will become part of the Crossrail service). The underground network of 402km is complemented with 167km and 57km of overground and TfL rail tracks, respectively.

Table 1 summarizes key topological indicators for the three networks. The London network is the largest in terms of both the number of nodes and links, followed by Shanghai (the Shanghai network analyzed by (Zhang et al. 2011) reflects the network state in 2010 and consisted of 240 stations and 264 links). Despite its size, the average number of intermediate stations that needs to be traversed when travelling between two stations is the lowest of all networks for London. Furthermore, the diameter (i.e. the length of the longest shortest path) is also the lowest in London. This can be explained by the greater connectivity of the London network as reflected in the relation between the number of links and ODs. The diameter of the Randstad network is considerably larger than in Shanghai, whereas the average shortest path is slightly shorter. Yet, even though the Shanghai network includes 30% more stations than the Randstad, the length of the average shortest path is less than 5% longer. This suggests that the Randstad network is the least efficient in terms of offering short travel alternatives between various OD pairs. This is further confirmed by the fact that the Randstad network has the longest diameter and the lowest value of average node degree centrality. The number of lines in the Randstad network is significantly higher than in Shanghai and London since it comprises of the local metro networks in Amsterdam and Rotterdam as well as parts of the national railway network which are operated by both intercity and local trains with distinctive stopping patterns.

Table 1: Summary of network topological indicators

Network	Number of nodes, $\|N\|$	Number of links, $\|E\|$	Number of lines, $\|L\|$	Average shortest path, $\bar{l}$	Diameter, $\max_{i,j} l(i,j)$	Average node degree centrality, $\bar{k_t}$
Shanghai	329	377	15	31.19	41	2.29
Randstad	254	283	66	29.86	46	2.23
London	368	427	12	26.54	36	2.32

4 RESULTS

An analysis of the characteristics and spatial distribution of centrality indicators in the three networks is first presented in section 4.1. Thereafter, the results of the disruption simulation and robustness analysis detailed in Section 2 for the networks of Shanghai, Randstad and London are presented in section 4.2.

4.1 Network centrality indicators

The simulated disruption scenarios are based on the dynamic update of degree and betweenness centrality rankings. Furthermore, network robustness is expected to depend on network properties and the availability of alternative routes, i.e. redundancy. It is therefore relevant to examine to what extent the networks differ in terms of the spatial variations in link and node centrality indicators as this can explain their performance under disruptive situations. Figures 1 and 2 display the degree (top) and betweenness (bottom) centrality indicators for the Shanghai (left), Randstad (middle) and London (right) networks, for node and links, respectively.

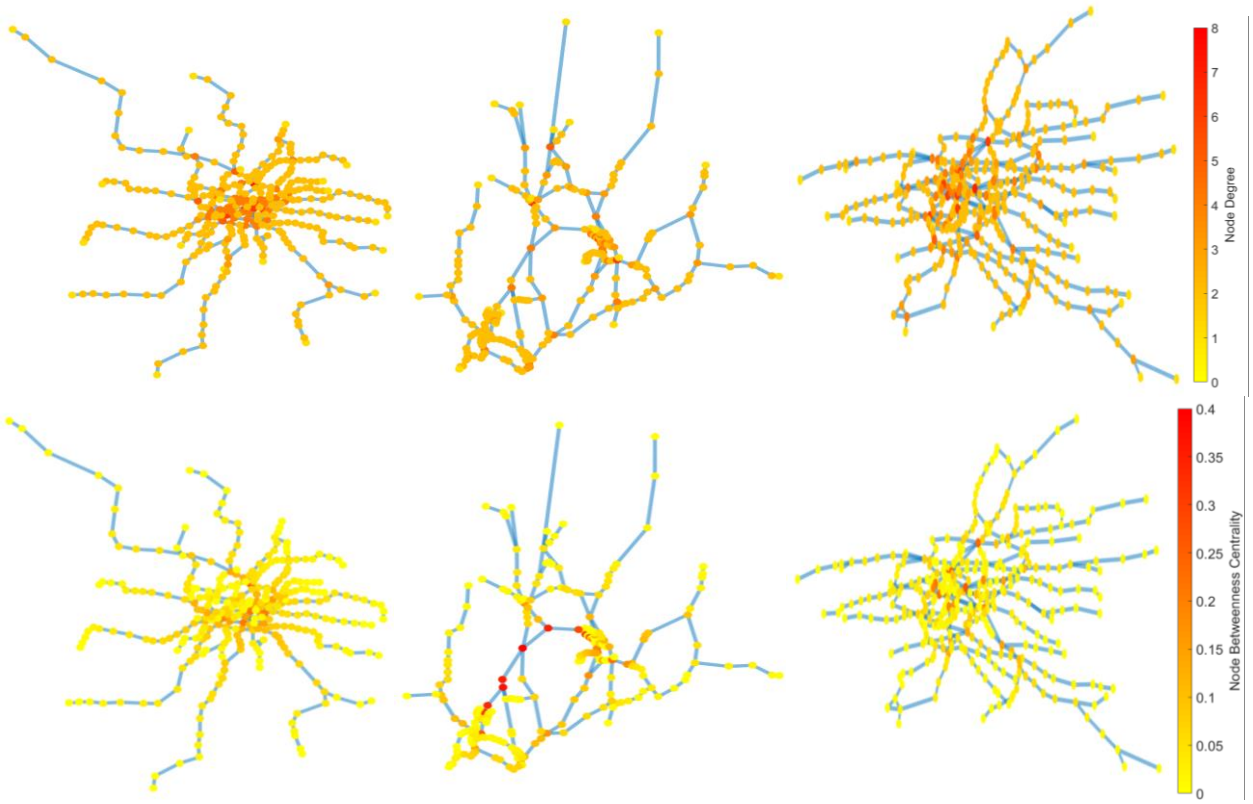

Figure 1: Node centrality indicators of the case study networks: Degree Centrality (above) and Betweenness Centrality (below); Shanghai (left), Randstad (middle) and London (right)

The Shanghai and London networks have a profoundly different structure than the Randstad as can be observed in Figures 1 and 2. The Shanghai and London networks have a typical radial structure, yet contain a finely meshed core with a large number of inner circuits. The London network has a large number of circuits also outside of the network core, offering additional possibilities for interchanging and cross-radial connections. The Randstad network in contrast has a less pronounced center and can be characterized as a grid network with some additional cycles around its main cities. These differences in network structure are clearly reflected in the distribution of node degree (Figure 1, top). The highest node degree values are all concentrated in the geographical core of the Shanghai network and to a lesser extent in the case of London. Conversely, the highest node degree values are scattered in the Randstad case, corresponding to key rail intersections, often located between rather than within dense urban areas (i.e. top three stations are Gouda, Woerden and Weesp, none of them in a major city or among the most frequently visited stations). The same pattern can be seen in relation to link degree (Figure 2, top).

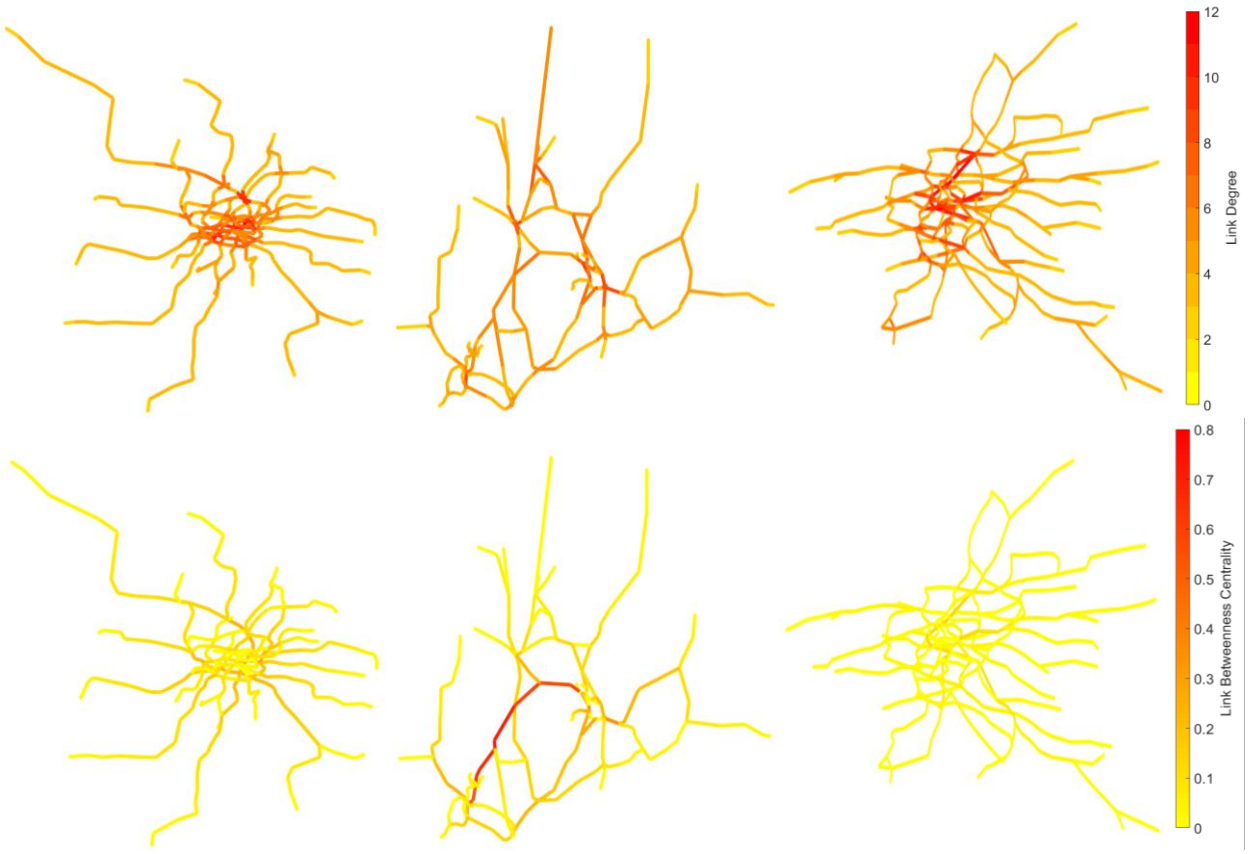

Figure 2: Link degree (above) and betweenness (below) centrality for Shanghai (left), Randstad (middle) and London (right)

Nodes with high betweenness centrality (Figure 1, bottom) are mostly located in the southeastern part of the Shanghai core, reflecting the center of gravity of the network as the shortest paths between most OD pairs traverse this part of the network. Conversely, nodes with high betweenness centrality in the Randstad network are situated along the main northeast-southwest axis which connects Amsterdam and Rotterdam, the two largest cities in this polycentric agglomeration. The same axis is clearly visible also when examining the link betweenness centrality (Figure 2, bottom). It is evident that link betweenness centrality is much more evenly distributed in the cases of Shanghai and London (note that the metric is displayed in relative terms, all values summing up to 1 for each network). This may suggest that the latter networks are more robust as they are not highly dependent on few selected links. As can be expected, there is a strong correspondence between node (Figure 1) and link (Figure 2) betweenness centrality values geographical disparity. Note that all to ease comparison across networks, we use the same scale for all networks. Due to the larger number of links in the London network than for the other two networks (Table 1), link betweenness centrality values (which sum up to one) are lower.

The variability of the centrality indicators is further investigated by plotting and comparing the distributions of both centrality indicators for both links and nodes for the three networks. While the node degree distributions are overall similar for all three networks, London and especially Shanghai exhibit higher link degree values (Figure 3, left). This indicates that nodes with a high degree value are more likely to be connected to other nodes with a high node degree in the London and Shanghai cases than in the Randstad case, creating 'cliques' of high degree nodes which are highly connected nodes as visible in Figure 1.

Both node and link betweenness centrality are very skewed for all networks (Figure 3, right). In all cases, few nodes and links are highly central in terms of them constituting part of the shortest path for a large share of the OD pairs, while the vast majority of nodes and links are on the shortest path of only few OD pairs. The Gini index (i.e. a measure of statistical dispersion ranging from zero for perfectly equal distribution to one for maximal inequality) of the node and link betweenness centrality values exceeds 0.89 for all networks for both node and link centrality. Notwithstanding, the Randstad network is less extremely skewed than London and Shanghai with Gini index values of 0.89 and 0.93 for node and link betweenness centrality, respectively. The corresponding values for London are 0.96 and 0.99 and for Shanghai 0.96 and 0.97.

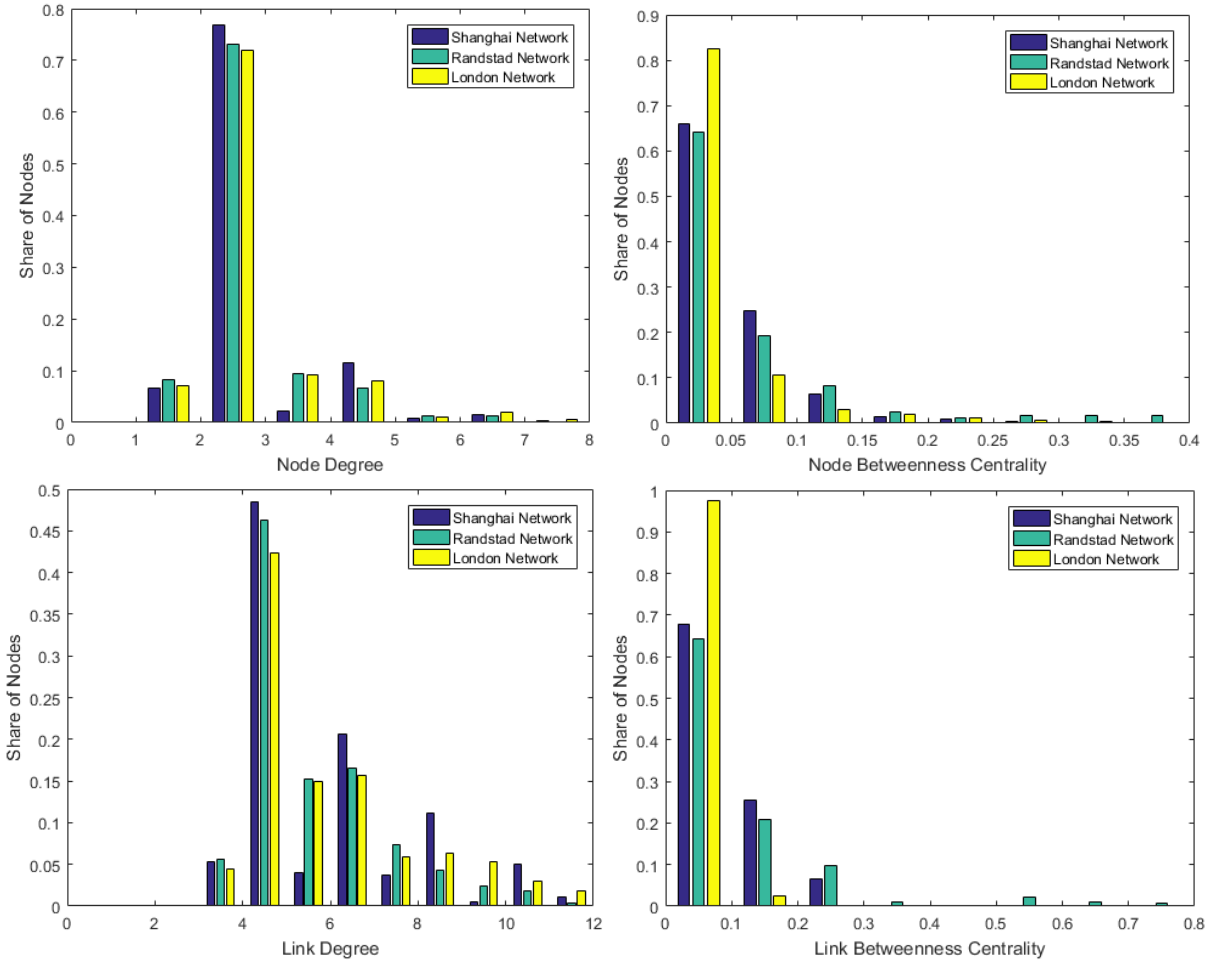

Figure 3: Comparison of node (above) and link (below) degree (right) and betweenness (left) centrality distributions for Shanghai, Randstad and London

The betweenness centrality distribution for the networks follow a power law distribution with an exponent defined as $k^{-\lambda}$ where k is the betweenness centrality and λ is the power law exponent. Figure 4 shows the node betweenness distribution and the corresponding power law fit. The λ values and R^2, i.e. the goodness-of-fit measure for the distribution fitting function, for the three networks is given in Table 1. All three networks can be characterized by a power law distribution of node betweenness centrality implying that few nodes serve a large share of passenger flows while many nodes serve a large share of the demand distribution. This may have consequences for local congestion effects and network robustness.

The Randstad network is the slightly less centralized than Shanghai and London as reflected by the lower exponent value.

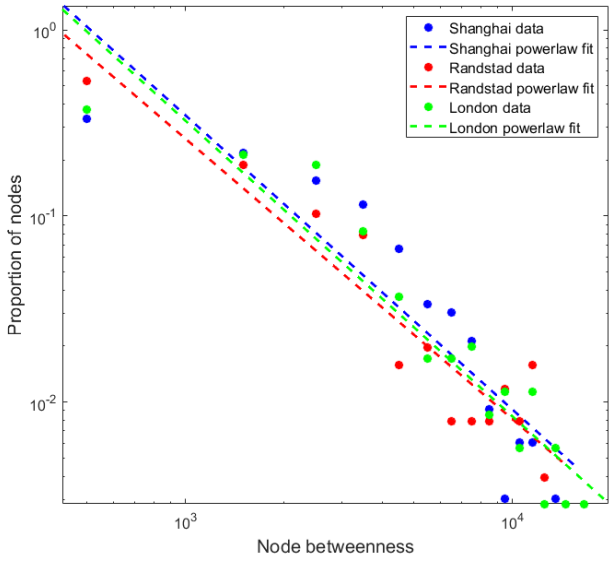

Figure 4: Log-log plot of node betweenness distribution for Shanghai, Randstad and London.

Table 1: Power law metric of node degree distribution per network

Network	λ	R^2
Shanghai	1.5808	0.7148
Randstad	1.5068	0.9611
London	1.5886	0.7677

4.2 Analysis of network performance deterioration path

Convergance patterns of the consequences of random attacks

As described in Section 2.2, the random network element removal strategy requires a number of simulation runs to obtain statistically significant results. Each simulation run involves a random sequence of nodes or links to be removed. We find that 300 iterations are sufficient to secure a 95% confidence level for all networks, scenarios and indicators. The convergence pattern of the network performance and robustness indicators for all three networks under node and link element failure scenarios can be observed in Figure 5.

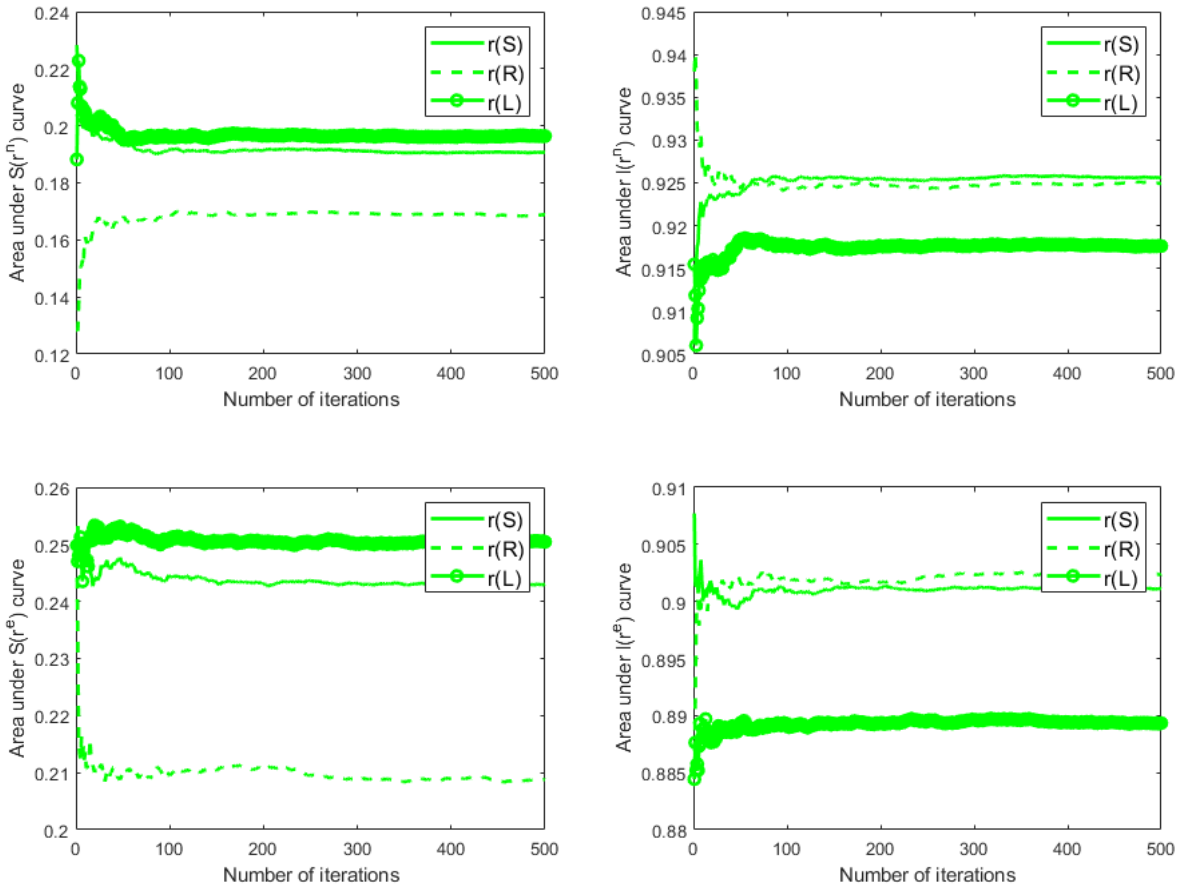

Figure 5: Convergence of Relative Size, S, (left) and Normalized Average Shortest Path, $\tilde{l}$, (right).under random node (above) and link (bottom) removal strategies in terms for the Shanghai (S), Randstad (R) and London (L) networks

Network performance and robustness in the event of successive node or link failures

The results of the node and link removal strategies are summarized in Figure 6. Each curve corresponds to the sequence of either link or node removal strategy by one of the removal sequences – based on degree (k), betweenness (b) or random attacks (RA) - for the Shanghai (S), Randstad (R) or London (L) network. In all cases, the curve starts from the value which corresponds to the initial undisrupted state of the network. In the case of the relative decrease in network performance in terms of the size of the largest connected component, S, the intial value is one – i.e. all networks form a single connected component in the undisrupted case. The share of this component is monotonically decreasing with a larger share of the nodes or links removed. Conversely, when measuring changes in the normalized average shortest path the value increases monotonically with the sequential removal of network elements.

The relative size of the largest component (Figure 6, left) decreases quickly and abruptly for all three networks considered when removing nodes or links by order of importance, especially when removing based on betweenness. Less than 18% of the OD pairs remain reachable, i.e. $S < 0.18$, after the top 5% most central nodes or 10% most central links in terms of betweenness centrality have been removed. This happens most quickly in the Randstad network followed by London, outperformed by Shanghai. A similar pattern albeit at a later point occurs when removing nodes or links by order of their degree centrality, obtaining the same levels of S after removing roughly twice as many elements (i.e. 10% of the nodes and 20% of the links). Hence, the pace of network deterioration when removing links based on betweenness is

twice as fast than when removal is based on degree. Hence, global connectivity is more important than local connectivity in determining the most critical links. Again, the Randstad is most vulnerable while in the case of sequential degree removal London and Shanghai perform similarly.

In contrast to the abrupt reduction in performance inflicted by removing sequentially the most central elements, a much slower and more gradual deterioration occurs when removing nodes or links randomly. After removing about 40% of the nodes or 50% of the links by order of their (degree or betweenness) centrality, the sub-networks are extremely fragmented with no sub-network consisting of more than 1% (up to 4 nodes or links) of the original graph. Conversely, this does not happen until the removal of 80% of the nodes or links when those are removed at random. The Randstad network is least robust to random failures while the London network outperforms Shanghai. All three networks are more robust to link removal than to node removal. This could be expected since the removal of a node involves the removal of all links connected to this node, hence resulting with a faster breakdown. Interestingly, random removal can be more harmful than targeted removal by degree when only few links are removed from the network (bottom left).

Overall, the patterns for the three networks follow a similar trend in terms of the relation between share of elements removed and size of the largest connected component. Notwithstanding, the performance of the Randstad network is clearly inferior to the Shanghai and London networks in the event or random node or link removals. The Randstad is also more pronouncedly underperforming in sequential link removals than when coping with sequential node removals as observed through larger S values under most shares of links removed (Figure 6, left). For example, after the removal of 10% of the links with the highest degree centrality, the Shanghai network is still connected, allowing travelling between any OD pair, while the largest connected sub-network in the Randstad lost more than 40% of the original network elements. However, after the removal of 15%, all networks are equally (dis)connected with $S \approx 5\%$.

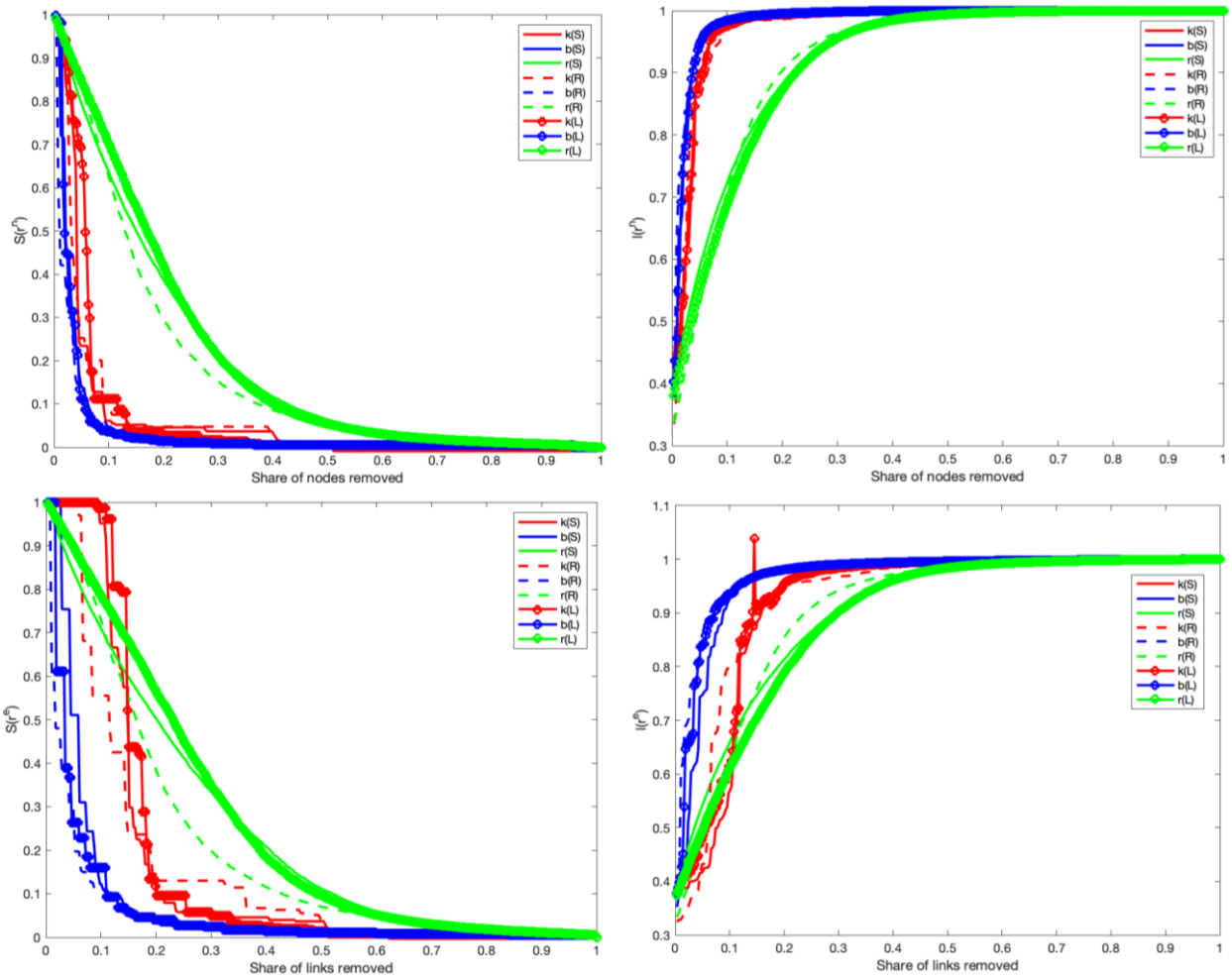

Figure 6: Shanghai (S), Randstad (R) and London (L) performance under alternative node (above) and link (bottom) removal strategies (k – node centrality; b – betweenness centrality; r –random) in terms of Relative Size, S, (left) and Normalized Average Shortest Path, $\tilde{l}$, (right).

Similar trends are observed for the normalized average shortest path length metric, $\tilde{l}$ (Figure 6, right). Again, all networks are much more vulnerable to targeted attacks than to random failures, with attacks targeting the network elements with the highest betweenness centrality values being the most devastating. In targeted removal scenarios, after only 5% of the nodes are removed, $\tilde{l}$ already approaches 0.9. Hence, even though both networks have not broken down yet ($S = 1$), severe detours are needed, resulting in significantly longer paths. No significant differences between the three networks are observed when removing nodes expect for a noticeable advantage for the London and Shanghai networks over the Randstad when 15-30% of the nodes have been randomly removed.

The Shanghai and London network are again superior to the Randstad network in terms of their robustness to link removal scenarios (Figure 6, bottom right). An interesting spike occurs for the London network when removing links by their degree which we further investigate. After removing 10% of the nodes or 20% of the links based on either degree or betweenness centrality, the network breakdown as indicated by the S metric is so severe, that the disconnected OD pairs dominate the normalized average shortest path calculations resulting with $\tilde{l}$ values approaching 1. This is in line with the findings of Chopra et al. (2016) which concluded that while the London metro system is robust to random breakdowns it is highly vulnerable to disruptions at selected critical stations. Conversely, this happens only after the

542 removal of 40% of the nodes or 50% of the links when those are removed at random. After the removal of
543 about 14% of the links, the detour required for travelling between certain OD pairs exceeds the diameter
544 in the original network, hence yielding $\tilde{l} > 1$. This is however not sustained after the next link is removed
545 as the ODs with the longest path in the previous network are not part of the same connected network
546 anymore.
547
548 For both node and link removal, removing network elements by order of their (updated) betweenness
549 centrality carries the most adverse consequences for both relative size and normalized average shortest
550 path indicators, followed by the removal based on degree centrality. Even though random removal is in
551 general the least harmful, it does initially result with more severe network *degradation* than targeted link
552 removal based on node degree (Figure 6, below). When comparing node and link removal, there are no
553 considerable differences in the event of random failures. In contrast, when removal is based on degree, node
554 failures yield more adverse network *degradation* conditions than link failures because node removal implies
555 removing all connected links (i.e. many for high degree nodes) and hence there are more adverse
556 consequences for the first removed nodes than for the first removed links. In the case of betweenness, again
557 node removal results with greater ramifications because it implies removing a number of links likely to be
558 along shortest paths of many ODs while for a link the removal concerns a single link. This difference
559 between node and link removals is especially visible for the Randstad network – more than for London and
560 Shanghai - because few links are more consequential given that the network offers relatively little
561 redundancy between the urban cores and the removal of a high degree or betweenness node implies the
562 removal of bypass alternatives.
563
564 *Aggregate metric of network robustness*
565 The analysis of the curves plotted in Figure 6 sheds light on the degrading rapidity of the three networks.
566 In addition, an aggregate metric of network robustness with respect to the largest connected component
567 (Eq. 8), A, is calculated for all scenarios. A is the integral of the curves plotted in Figure 6, left. Hence, an
568 extremely vulnerable network which breaks apart instantly after the first node or link has been removed
569 will yield $A = 0$. In contrast, the hypothetical case of an extremely robust network that remains intact
570 until the very last brick is removed will yield $A = 1$.
571
572 The results in Table 2 show that the Randstad is consistently the least robust with considerably lower
573 overall scores than London and Shanghai under all removal scenarios. London outperforms Shanghai when
574 considering removal by node or link degree as well as random failures whereas Shanghai is most robust to
575 removals based on betweenness centrality values, especially in the case of link-based attacks.
576
577 The results in Table 2 also highlight that network robustness differs more by the removal strategy than
578 among the extent to which it varies among the case study networks. For the same removal selection
579 criterion, networks are more robust to link removals than to node removals by approximately 25, 100 and
580 175 % for random, betweenness and degree, respectively.
581

582
583 Table 2 : Aggregate metric of network robustness per scenario and network

Network	Node removal			Link removal		
	node degree (k)	*node betweenness centrality (b)*	*random (r)*	*link degree (k)*	*link betweenness centrality (b)*	*random (r)*
Shanghai	5.64	3.42	19.11	16.22	7.24	24.33
Randstad	5.54	2.97	16.82	14.95	5.06	20.76
London	6.22	3.41	19.99	17.17	5.79	25.60

584

585 **4.3 Network performance and robustness in the event of line closures upon node or link failure**

586 We now turn to examining the set of scenarios where the failure of a network element implies the closure
587 of all lines traversing the respective element. The three removal strategies are tested for the three case study
588 networks. The convergence pattern in the event of line closure follows similar convergence trends to those
589 reported in Figure 5. Similarly to Figure 6, each curve in Figure 7 corresponds to the sequence of either link
590 or node removal strategy by one of the removal sequences, though in the event that a node or link failure
591 implies that all lines traversing the respective station or track segment break down. Note that the x-axis
592 displays the number of iterations (i.e. absolute number of elements removed) rather than the share of nodes
593 or links removed since here the removal of a node or link implies the removal of additional nodes and links
594 which are served by the same line(s).
595
596 Figure 7 displays the results degree (k), betweenness (b) or random attacks (RA) - for the Shanghai (S),
597 Randstad (R) or London (L) network. When comparing the results shown in Figure 7 to those of Figure 6
598 it can be seen that node failures result in considerably more adverse conditions in the event of line
599 operation failures for all networks. This is expected because the removal of a node implies the removal of
600 all other stations serviced by the same line. Moreover, the removal of many of the nodes involves the closure
601 of several lines, especially in the case of non-random removal strategies since central nodes often been
602 serviced by more than one line. This results with an accelerated network fragmentation where the removal
603 of a handful of central nodes or 20 random nodes already results with the largest connected component
604 consisting of less than 10% of the original network ($S < 0.1$). No significant differences are observed
605 among the case study networks whereas the removal strategy is determines network degradation
606 trajectory. Unlike in Figure 6, the removal strategy based on node degree centrality is more consequential
607 than node betweenness centrality since here it implies the removal of not only the directly connected links
608 but all nodes and links served by common lines.
609
610 Similar to the analysis in the previous sub-section, link failures are less adverse than node failures. This
611 difference is more pronounced in the event that removals result with line closures (Figure 7) since node
612 removals imply now not only the removal of all connected links but also all upstream and downstream
613 nodes and links on all lines traversing these links, further exacerbating network degradation. Conversely,
614 link removal implies only the removal of all lines serving this specific link. Yet, network degradation
615 process is of course accelerated when compared with the scenarios where lines remain operational. For
616 example, the largest sub-component S is smaller than 0.1 after the removal of 18 links for all networks and
617 scenarios – amounting to less than 7% of the links for all networks, whereas $S > 0.6$ for all random and
618 degree removing scenarios for the respective share of links removed for all networks (Figure 6, bottom left).

In the event of link failures followed by line closures, considerably different network degradation patterns can be observed. The Randstad network is most vulnerable to removal strategies based on either degree or betweenness in terms of both the relative size and average normalized shortest path. This can be explained by the large number of lines traversing central links. At the same time, the Randstad network also has the longest tail implying that the network has not completely degraded even after the removal of the same number of links which results with complete fragmentation in the larger networks of Shanghai and London. Upon further investigation it appears that this long tail stems from the locally connected metro networks which are embedded in the Randstad network. The London and Shanghai networks exhibit similar patterns in the event of targeted – either degree or betweenness centrality based – attacks. In contrast, while the London network performs similarly also in the event of random and targeted attacks, the Shanghai network is more robust to random failures and hence more robust than the London network to such failures.

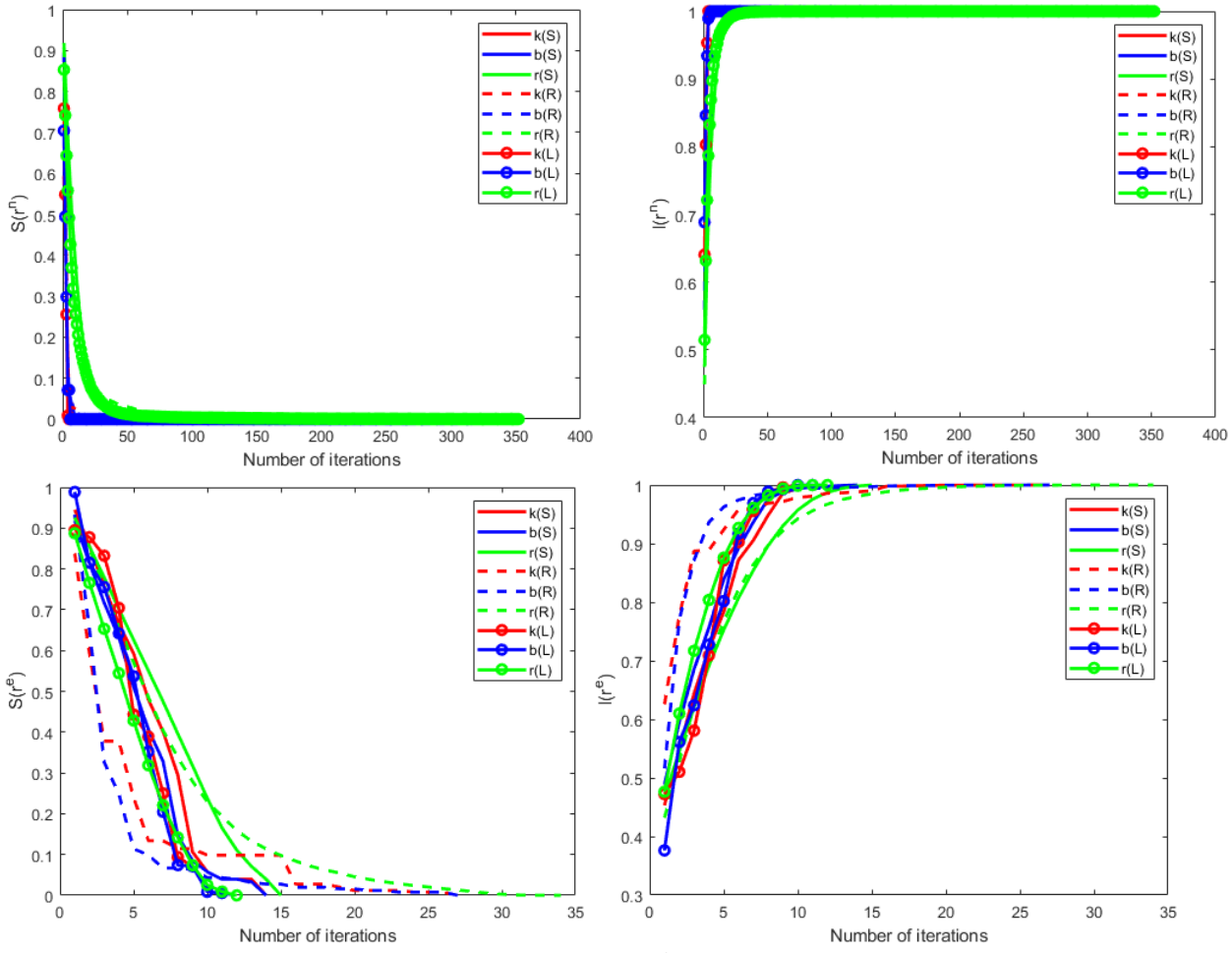

Figure 7: Shanghai (S), Randstad (R) and London (L) performance under alternative node (above) and link (bottom) removal strategies (k – node centrality; b – betweenness centrality; r –random) with service line closures in terms of Relative Size, S, (left) and Average Normalized Shortest Path, $\tilde{l}$, (right).

5 DISCUSSION AND CONCLUSION

In this paper, a network vulnerability analysis is performed for Shanghai, Randstad and London heavy rail networks. The three networks possess different structures: a recent and rapidly developing network serving a monocentric metropolitan area, an exemplary of a polycentric urban agglomeration area that has

developed over many decades by a large number of planning authorities and a monocentric network with a centralized planning authority that has developed since gradually since the late 19th century. Our findings confirm that network structure properties results with different robustness perofrmances. Both link-based and node-based sequential removal are applied to test the network and the performance of the degraded network is measured in terms of the relative size of the largest component (S), the relative mean shortest path ($\tilde{l}$) and an aggregate robustness measure (A). Random failures as well as targeted attacks based on degree and betweenness centrality are examined. We assess network robustness in case failures are confined to the disrupted node or link as well as in the case that local breakdown imply that line operations are hindered. In the latter case, the fragmentation of the network happens much more rapidly. Furthermore, networks are 25-175 % more robust to link than to node removals.

The results of this study shed new light on some of the common conventions held in the network robustness discourse. The polycentric network of the Randstad was found the least robust in this analysis when compared to the more monocentric networks of London and Shanghai. Unlike what might be expected, the network polycentricism does not yield in the case of the Randstad with a more distributed hub and spoke structure that is known to contribute to network robustness but rather results in few key stations and tracks that lie outside of the urban cores in a fork-like structure. The network is fragile to breakdowns of tracks and stations that are between key centers. Examples of which include the connection between the airport and seaport areas (both among the largest in Europe and key national infrastructure) and the connection between the seat of government and center of public administration (The Hague) and the capital and financial center (Amsterdam). The structure of the Randstad network echoes the common saying about the Dutch agglomeration – it is not a dense country but rather an empty city. Consequently, the poorly meshed core offers few rerouting possibilities in the event of disruption, resulting with a quick fragmentation of the network in the event of sequential failures. This is further exacerbated by the presence of a large number of lines traversing central links.

The Shanghai and London networks offer redundancy especially in their finely meshed cores. The London network is in general more robust than the Shanghai network thanks to the presence of cycles beyond the core especially in the southern and northern boroughs. A closer inspection reveals that the Shanghai network includes relatively more and longer branches spreading out of the core, while London has more peripheral hub connections. It is well-known that the connectivity of radial networks is highly vulnerable to disruption, isolating one branch from the remaining network.

This study has several implications for network planning and design. First, the robustness of polycentric regions highly depends on the availability of routing alternatives between the most populated areas. Due to lower densities between the urban cores, networks serving polycentric areas may rely on a limited number of connecting corridors. This however has severe consequences for network robustness as their malfunction will result with an immediate breakdown and loss of a significant share of network functionality. Second, a finely meshed network core cannot substitute the availability of connections between outer hubs, in the absence of which long branches can become disconnected without any viable alternative. Planning as well as further research may consider the redundancy offered by alternative public transport modes in metropolitan regions as well as the service properties such as occupancy and capacity associated with them. Network design, including the design of public transport network, involves striking a balance between efficiency and robustness. Hence, the introduction of additional network redundancy in the form of new links that create cycles depend on their utilization under normal conditions (shortening travel times, relieving congestion) as well as the ability to absorb demand in the event of disruptions on alternative routes (Jenelius and Cats 2015).

Our findings suggest that the relation between network structure and its robustness is non-trivial. While in general more decentralized networks are more robust to targeted attacks, a polycentric urban agglomeration does not necessarily yield a more distributed network as measured in terms of centrality

indicators. Furthermore, there is also no indication that a rapid and presumably more top-down centralized development necessarily results with a more robust design. An organic and less centralized development may result with lesser concentration of the rail network. It may thus be the case that a bottom-up and lengthy development may result with more fractal-like geometry due to underlying network evolutionary principles as indicated by empirical research of the evolution of road networks in Italy and Paris (Strano et al. 2012, Barthélemy et al. 2013). The growth process has been characterized by an expansion phase where branches are built into areas previously not served by roads followed by a densification phase where the network became denser through the addition of links between already existing branches.

Further research is needed in order to examine the generality of the results presented in this study, related processes and their consequences for network design as well as the incorporation of demand patterns and service properties. Statistical relations between network topology and passenger flow distribution may allow the systematic comparison of networks worldwide even in the absence of publicly available data concerning public transport demand (Luo et al. 2019). Future studies may thus investigate network robustness while considering infrastructure utilization, the residual capacity and the availability and quality of routing alternatives for rolling stock (Gahemi et al. 2018a) as well as passengers (Gahemi et al. 2018b). The results of the robustness analysis performed in this study neglect the constrained operational environment that characterizes railway systems and the limited information available to passengers when encountering service disrputions (Cats and Jenelius 2014). A detailed and dynamic analysis which includes the representation of vehicle and passenger flows will allow attaining a more realistic assessment. Notwithstanding, the network science approach offers a powerful tool to systematically compare large-scale networks with very limited input specifications requirements. While such analysis can lead to insightful observations and global patterns, it simplifies many aspects that are important for devising planning and operational measures. Furthermore, passenger demand may be included in robustness assessment, allowing the consideration of the number of passengers affected by various disruptions (Cats 2016). Another direction for further research is the propagation of network failures in the event of natural disasters as governed by spatial correlations (Wisetijndawat et al. 2019) and its impacts for resilience under alternative network structures.

ACKNOWLEDGEMENT

Part of this work was funded by the European Union's Horizon 2020 SETA project under the grant agreement No 688082.

REFERENCES

Ash, J. and Newth, D. (2007). Optimizing complex networks for resilience against cascading failure. *Physica A* 380, 673-683.

Barthélemy M., Bordin P., Berestycki H. and Gribaudi M. (2013). Self-organization versus top-down planning in the evolution of a city. *Scientific Reports*, 3, 2153.

Cats, O. (2016). The robustness value of public transport development plans. *Journal of Transport Geography*, 51, 236-246.

Cats, O. (2017). Topological evolution of a metropolitan rail transport network: The case of Stockholm. *Journal of Transport Geography*, 62, 172-183.

Cats O. and Jenelius E. (2014). Dynamic vulnerability analysis of public transport networks: Mitigation effects of real-time information. *Networks and Spatial Economics*, 14, 435-463.

Cats O., Koppenol, G-J. and Warnier M. (2017). Robustness assessment of link capacity reduction for complex networks: Application for public transport systems. Reliability Engineering & System Safety, 167, 544-553.

Cats, O., Wang, Q. and Zhao, Y. (2015). The identification and classification of urban centres using public transport passenger flows data. *Journal of Transport Geography*, 48, 10-22.

Chopra S.S., Dillon T., Bilec M.M. and Khanna V. (2016). A network-based framework for assessing infrastructure resilience: a case study of the London metro system. *Journal of the Royal Society Interface*, 13 (118): 20160113.
Derrible, S., Kennedy, C. (2010a). Characterizing metro networks: state, form and structure. *Transportation*, 37, 275-297.
Derrible, S., Kennedy, C. (2010b). The complexity and robustness of metro networks. *Physica A*, 389, 17, 3678-3691.
Gallotti, R., Porter, M. A., and Barthelemy, M. (2016). Lost in transportation: Information measures and cognitive limits in multilayer navigation. *Science advances*, 2(2), e1500445.
Ghaemi, N., Cats, O. and Goverde, R.M.P. (2018). Macroscopic multiple-station short-turning model in case of complete railway blockages. *Transportation Research Part C*, 89, 113-132.
Homeland Security, U.S. Department of (2010). Transportation Systems Sector-Specific Plan, an Annex to the National Infrastructure Protection Plan.
Jenelius, E. and Cats, O. (2015). The value of new public transport links for network robustness and redundancy. *Transportmetrica A*, 11 (9), 819-835.
Ghaemi N., Cats O. and Goverde R.M.P. (2018a). Macroscopic multiple-station short-turning model in case of complete railway blockages. *Transportation Research Part C*, 89, 113-132.
Ghaemi N., Zilko A., Yan F., Cats O., Kurowicka D. and Goverde R.M.P. (2018b). Impact of Railway Disruption Predictions and Rescheduling on Passenger Delays. *Journal of Rail Transport Planning & Management*. Accepted.
Latora, V., and Marchiori, M. (2001). Efficient behavior of small-world networks. *Physical review letters*, 87(19), 198701.
Lin, J., and Ban, Y. (2013). Complex Network Topology of Transportation Systems. *Transport Reviews*, 33(6), 658-685.
Louf, R. and Barthelemy, M. (2013). Modeling the polycentric transition of cities. *Physical Review Letters*, 111.
Luo D., Cats O. and van Lint H. (2019). Can passenger flow distribution be estimated solely based on network properties in public transport systems? *Transportation*, 1-20.
Malandri C., Fonzone A. and Cats O. (2018). Recovery time and propagation effects of passenger transport disruption. *Physica A*, 505, 7-17.
Pagani A., Mosquera G., Alturki A., Johnson S., Jarvis S., Wilson A., Guo W. and Varga L. (2019). Resilience or robustness: identifying topological vulnerabilities in rail networks. *Royal Society Open Science*, 6 (2), 1-16.
Rodriguez-Nunez, E. and Garcia-Palomares, J.C. (2014). Measuring the vulnerability of public transport networks. *Journal of Transport Geography*, 35, 50-63.
Roth, C., Kang, S. M., Batty, M. and Barthelemy, M. (2012). A long-time limit for would subway networks. *Journal of the Royal Society Interface*, 9, 2540-2550.
Sen, P., Dasgupta, S., Chatterjee, A., Sreeram, P. A., Mukherjee, G., and Manna, S. S. (2003). Small-world properties of the Indian railway network. *Physical Review E*, 67(3), 036106.
Strano,E., Nicosia, V., Latora, V., Porta, S. and Barthelemy, M. (2012). Elementary processes governing the evolution of road networks. *Scientific Reports*, 2, 296.
von Ferber, C., Berche, B., Holovatch, T., and Holovatch, Y. (2012). A tale of two cities. *Journal of Transportation Security*, 5(3), 199-216.
von Ferber, C., Holovatch, T., Holovatch, Y., and Palchykov, V. (2009). Public transport networks: empirical analysis and modeling. *The European Physical Journal B*, 68(2), 261-275.
Wang, Z., Chan, A. P., Yuan, J., Xia, B., Skitmore, M., and Li, Q. (2014). Recent advances in modeling the vulnerability of transportation networks. *Journal of infrastructure systems*, 21(2), 06014002.
Wang, X., Koc, Y., Derrible, S., Ahmad, S.N., Pino, W.J.A. and Kooij, R.E. (2017). Multi-criteria robustness analysis of metro networks. *Physica A*, 474, 19-31.

790 Wang, J., Jin, F., Mo, H. and Wang, F. (2009) Spatiotemporal evolution of China's railway network in the
791 20th century: An accessibility approach. *Transportation Research Part A*, 43 (8), 765-778.
792 Wisetijndawat, W., Eddie Wilson, R., Bullock, S. and de Villafranca, A.E.M. (2019). Modeling the impact
793 of spatial correlations of road failures on travel times during adverse weather conditions. *Transportation*
794 *Research Record*, 2673(7), 157-168.
795 William, M.J. and Musolesi, M. (2016). Spatio-temporal networks: reachability, centrality and robustness.
796 *Royal Society Open Science*, 3 (6), 1-20.
797 Zhang, X., Miller-Hooks, E. and Denny, K. (2015). Assessing the role of network topology in transportation
798 network resilience. *Journal of Transport Geography*, 46, 35-45.
799 Zhang, J., Xu, X. And Hing, L. (2011). Networked analysis of the Shanghai subway network, in China.
800 *Physica A*, 390, 4562-4570.
801